

HOW TO INTERCONNECT FOR MASSIVE MIMO SELF-CALIBRATION?

Fuqian Yang¹, Hanyu Zhu¹, Cong Shen², Linglong Dai³, and Xiliang Luo¹

¹ShanghaiTech University, ²University of Science and Technology of China, ³Tsinghua University

ABSTRACT

In time-division duplexing (TDD) systems, massive multiple-input multiple-output (MIMO) relies on the channel reciprocity to obtain the downlink (DL) channel state information (CSI) with the acquired uplink (UL) CSI at the base station (BS). However, the mismatches in the radio frequency (RF) analog circuits at different antennas at the BS break the end-to-end UL and DL channel reciprocity. To restore the channel reciprocity, it is necessary to calibrate all the antennas at the BS. This paper addresses the interconnection strategy for the internal self-calibration at the BS where different antennas are interconnected via hardware transmission lines. Specifically, the paper reveals the optimality of the star interconnection and the daisy chain interconnection respectively. From the results, we see the star interconnection is the optimal interconnection strategy when the BS are given the same number of measurements. On the other hand, the daisy chain interconnection outperforms the star interconnection when the same amount of time resources are consumed. Numerical results corroborate our theoretical analyses.

Index Terms— Calibration, Self-calibration, Interconnection, TDD reciprocity, massive MIMO.

1. INTRODUCTION

In massive multiple-input multiple-output (MIMO), a large number of antennas are installed at the base station (BS) to enhance the system spectral efficiency [1]. To avoid the need to feed back a large amount of downlink (DL) channel state information (CSI) to the BS as in frequency-division duplexing (FDD) systems, time-division duplexing (TDD) is typically assumed for massive MIMO where the channel reciprocity can be exploited to infer the DL CSI with the uplink (UL) CSI acquired at the BS [2]. However, in practice, the transmit and receive branches are composed of totally different analog circuits. Accordingly, the radio-frequency (RF) gain of the transmit chain is different from that of the receive chain at the base-band [3]. These RF gain mismatches destroy the end-to-end TDD channel reciprocity and lead to severe performance degradation in massive MIMO systems [3–5]. Careful calibration is thus necessitated to compensate those RF gain mismatches at the RF front ends (FEs) to restore the end-to-end UL/DL channel reciprocity.

There are two main categories of calibration schemes to compensate the RF gain mismatches. One is the “relative calibration” and the other one is the “full calibration”. The relative calibration was proposed to only restore the end-to-end UL and DL channel reciprocity without addressing the absolute phase or amplitude coherence [6]. On the other hand, the full calibration provides full absolute phase and amplitude coherence between transmitters and receivers [7].

To accomplish either the relative calibration or the full calibration, either the “Self-Calibration” scheme [5–10] or the “Over-The-Air (OTA)” calibration scheme [11–14] can be applied. By utilizing hardware interconnections with transmission lines [7–9] or ex-

ploiting the mutual coupling effects [5, 6, 10], the self-calibration scheme can be performed by the BS only without invoking helps from the served mobile stations (MSs) or other antenna arrays. The OTA calibration scheme is carried out with the help of the assisting MSs or other antenna arrays [13]. In massive MIMO, the OTA scheme usually requires a significant amount of CSI feedback from the MSs [14].

In this paper, we focus on the internal self-calibration scheme and seek for the optimal interconnection strategy to wire the antennas at the BS together with transmission lines. In particular, we analyze the optimality of the star interconnection and the daisy chain interconnection respectively under different resource constraints. The derived results in this paper can serve as the design guidelines for massive MIMO systems.

The rest of the paper is organized as follows. Section 2 gives the system model and performance characterization for self-calibration. Section 3 analyzes the optimality of the star interconnection strategy without considering the constraint on the time resources. Section 4 shows the optimality of the daisy chain interconnection strategy when the time resources are limited. Numerical results are provided in Section 5 and Section 6 concludes the paper.

Notations: $\text{Diag}\{\cdot\}$ denotes the diagonal matrix with the diagonal elements defined inside the curly brackets. Notations $\text{Tr}\{\cdot\}$, $(\cdot)^T$, $(\cdot)^H$, $(\cdot)^*$, and $|\mathcal{C}|$ stand for matrix trace, transpose operation, Hermitian operation, conjugate operation, and the cardinality of the set \mathcal{C} , respectively. $\mathcal{A} \setminus \mathcal{B}$ means the relative complement of the set \mathcal{B} in the set \mathcal{A} . $\text{mod}(a, b)$ represents modulo operation that finds the remainder after division of a by b . $[\mathbf{A}]_{p,q}$ denotes the (p, q) -th entry of matrix \mathbf{A} .

2. SYSTEM MODEL & CALIBRATION PERFORMANCE

2.1. System Model

Consider a TDD multi-user (MU) massive MIMO system with an M -antenna BS and U single-antenna MSs. As many works have shown, only calibration of the BS front-ends is required and the effects of RF gains at the MSs can be neglected [5, 7]. To obtain calibration coefficients at the BS, the self-calibration method with hardware circuit connection is considered in this paper [7]. The complex-valued transmit and receive RF gains of the antennas at the BS are denoted as $\{\alpha_m, \beta_m\}_{m=1}^M$. During the calibration phase, the BS antennas transmit sounding signals over the transmission lines to obtain calibration measurements. Let $y_{p,q}$ denote the received signal at the p -th antenna due to the transmission from the q -th antenna. Without loss of generality, the transmitted sounding signal is assumed to be 1. It then follows that

$$y_{p,q} = \beta_p h_{p,q} \alpha_q + n_{p,q}, \quad (1)$$

where $h_{p,q}$ represents the gain of the calibration channel between the p -th antenna and the q -th antenna and $n_{p,q}$ is the additive white Gaussian noise (AWGN) with zero mean and variance σ_n^2 . Note that

$h_{p,q} = 0$ if there is no interconnection wiring between the p -th antenna and the q -th antenna and $h_{p,q} = h_{q,p}$ due to the reciprocity of the calibration channel. Note that every transmission line is bidirectional and two measurements are obtained with each transmission line. By stacking all the calibration measurements in (1) together, the received signals in matrix-form is

$$\mathbf{Y} = \mathbf{R}\mathbf{H}\mathbf{T} + \mathbf{N}, \quad (2)$$

where $[\mathbf{Y}]_{p,q} := y_{p,q}$, $\mathbf{R} := \text{Diag}\{\beta_1, \beta_2, \dots, \beta_M\}$, $\mathbf{T} := \text{Diag}\{\alpha_1, \alpha_2, \dots, \alpha_M\}$, $[\mathbf{H}]_{p,q} := h_{p,q}$, and $[\mathbf{N}]_{p,q} := n_{p,q}$.

2.2. Performance Characterization

In this study, we only focus on the full calibration schemes, but similar results can also be derived when the relative calibration is considered. To restore the end-to-end channel reciprocity, the BS only need to know the values of those transmit and receive RF gains subject to a common scaling, e.g. $\{s_\alpha \alpha_m\}_{m=1}^M$ and $\{s_\beta \beta_m\}_{m=1}^M$. In order to proceed with our quantitative analyses, we assume there is a “reference antenna”, e.g. the f -th antenna, whose RF gains: α_f and β_f are known [10]. The other antennas are called “ordinary antennas” accordingly. For a particular interconnection strategy, given all the measurements \mathbf{Y} in (2), the corresponding Cramer-Rao low bounds (CRLBs) for those unknown calibration coefficients, i.e. $\{\alpha_m, \beta_m\}_{m=1}^M \setminus \{\alpha_f, \beta_f\}$, can be derived. Note these CRLBs serve as lower bounds for the variances of the estimation errors of all possible unbiased estimators [15]. Let the matrix \mathcal{A} represent the interconnection strategy. Specifically, it is defined as

$$\mathcal{A}_{p,q} := \begin{cases} 1, & \text{Antenna-}p, q \text{ are interconnected} \\ 0, & \text{otherwise} \end{cases}. \quad (3)$$

And let $\bar{\mathcal{A}}$ be the submatrix obtained by removing the f -th row and the f -th column from the interconnection matrix \mathcal{A} . In this paper, we endeavor to find the optimal interconnection strategy or wiring at the BS which connects different antennas in the most efficient way to enable the best estimates of the calibration coefficients. To proceed with our derivations, we make the following assumption:

- **AS-1:** All the transmission lines have the same length and damping, i.e. $h_{p,q} = h$ when the p -th antenna and the q -th antenna are interconnected.

Let $\boldsymbol{\theta}$ be a $2(M-1)$ -by-1 unknown vector defined as $\boldsymbol{\theta} := [\boldsymbol{\alpha}^T, \boldsymbol{\beta}^T]^T$, where $\boldsymbol{\alpha} := [\alpha_1, \dots, \alpha_{f-1}, \alpha_{f+1}, \dots, \alpha_M]^T$ and $\boldsymbol{\beta} := [\beta_1, \dots, \beta_{f-1}, \beta_{f+1}, \dots, \beta_M]^T$. According to the signal model in (2), under AS-1, we have $\mathbf{H} = h\mathcal{A}$ and the CRLB matrix for $\boldsymbol{\theta}$ with an interconnection strategy \mathcal{A} can be derived as [15]

$$\text{CRLB}(\boldsymbol{\theta}|\mathcal{A}) = \mathbf{J}^{-1}(\boldsymbol{\theta}), \quad (4)$$

where the Fisher information matrix $\mathbf{J}(\boldsymbol{\theta})$ is given by

$$\mathbf{J}(\boldsymbol{\theta}) = \frac{|h|^2}{\sigma_n^2} \cdot \begin{bmatrix} \mathbf{A} & \mathbf{D}^H \\ \mathbf{D} & \mathbf{B} \end{bmatrix}, \quad (5)$$

with

$$\begin{aligned} \mathbf{D} &:= \text{Diag}\{\boldsymbol{\beta}\} \cdot \bar{\mathcal{A}} \cdot \text{Diag}\{\boldsymbol{\alpha}^*\}, \\ \mathbf{A} &:= \text{Diag}\left\{ \sum_{i \in \mathcal{C}_1} |\beta_i|^2, \dots, \sum_{i \in \mathcal{C}_m, m \neq f} |\beta_i|^2, \dots, \sum_{i \in \mathcal{C}_M} |\beta_i|^2 \right\}, \\ \mathbf{B} &:= \text{Diag}\left\{ \sum_{i \in \mathcal{C}_1} |\alpha_i|^2, \dots, \sum_{i \in \mathcal{C}_m, m \neq f} |\alpha_i|^2, \dots, \sum_{i \in \mathcal{C}_M} |\alpha_i|^2 \right\}, \end{aligned} \quad (6)$$

and \mathcal{C}_m denotes the set of the indices of the antennas that are interconnected to the m -th antenna directly in this particular interconnection strategy \mathcal{A} . In this paper, we call an interconnection path

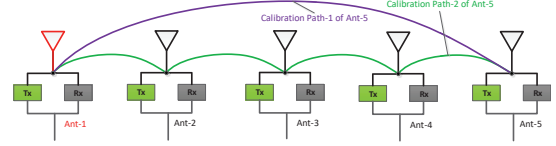


Fig. 1. The interconnection strategy with 5 antennas. Antenna-1 is chosen as the reference antenna and there are two calibration paths for antenna-5.

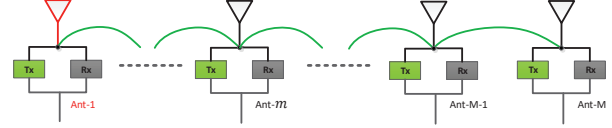


Fig. 2. The daisy chain interconnection strategy with M antennas. “Ant- f ” is the reference antenna, and number of antennas along the calibration path of the m -th antenna in addition to the reference antenna is d_m .

between one ordinary antenna and the reference antenna a “calibration path”. For example, the purple path shown in Fig. 1 is one calibration path of antenna-5. Note that to be able to estimate all the calibration coefficients, the chosen interconnection strategy \mathcal{A} must be “effective” in the sense that there must be at least one calibration path between each ordinary antenna and the reference antenna. Besides, to ensure an effective interconnection strategy, the BS must be equipped with at least $(M-1)$ transmission lines and at least $2(M-1)$ calibration measurements need to be obtained. In the following sections, the optimality of different interconnection strategies is analyzed based on the corresponding CRLBs for the unknown calibration coefficients.

3. OPTIMALITY OF THE STAR INTERCONNECTION

To gain more insights from the CRLB results in (4), we further make the following assumption:

- **AS-2:** The transmit and receive RF gains exhibit equal amplitudes, i.e. $|\alpha_m| = a, |\beta_m| = b, \forall m \in [1, M]$.

AS-2 is made mainly due to the following concern. Constant transmit and receive amplitudes ensure identical receive signal-to-noise ratio (SNR) in the calibration measurements at each BS antenna. The current study only focuses on the impact of the internal interconnection strategy. Assuming that the BS has a total budget of $(M-1)$ transmission lines to interconnect different antenna ports at the BS, under AS-2, closed-form expressions for the CRLBs in (4) can be derived. Further, the optimal interconnection strategies for internal full calibration can be characterized according to the derived analytical results.

To derive the closed-form CRLB expressions, we consider the daisy chain interconnection strategy as shown in Fig. 2, where the reference is set to $f = 1$. According to (5), under AS-1 and AS-2, the Fisher information matrix for the daisy chain interconnection strategy with M antennas is given as

$$\mathbf{J}_{\text{daisy}}(\boldsymbol{\theta}) = \frac{|h|^2}{\sigma_n^2} \cdot \begin{bmatrix} \mathbf{A} & \mathbf{D}^H \\ \mathbf{D} & \mathbf{B} \end{bmatrix}, \quad (7)$$

where

$$\begin{aligned} \mathbf{A} &= 2b^2 \cdot \text{Diag}\{1, 1, \dots, 1, 1/2\}, \\ \mathbf{B} &= 2a^2 \cdot \text{Diag}\{1, 1, \dots, 1, 1/2\}, \end{aligned} \quad (8)$$

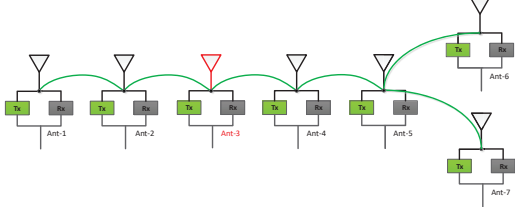


Fig. 3. An interconnection network with 7 antennas. The antenna-3 is chosen as the reference antenna.

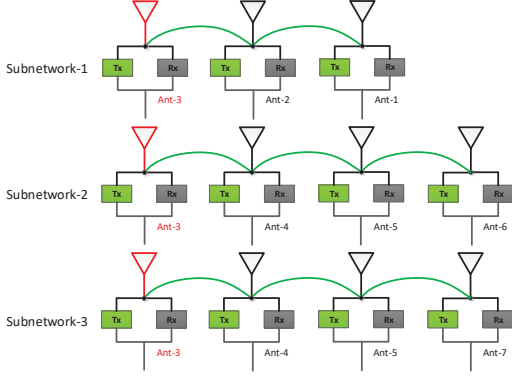


Fig. 4. The three decoupled interconnection subnetworks of the interconnection network in Fig. 3. The three subnetworks are all the daisy chain interconnection networks.

$$[\mathbf{D}]_{p,q} = \begin{cases} \beta_{p+1}\alpha_{q+1}^*, & |p-q|=1 \\ 0, & \text{otherwise} \end{cases}, \quad (9)$$

with $p, q \in [1, M]$. Hence, the diagonal elements of the matrix $\mathbf{J}_{\text{daisy}}^{-1}(\boldsymbol{\theta})$ can be directly obtained according to the inverse of the partitioned matrix $\mathbf{J}_{\text{daisy}}(\boldsymbol{\theta})$. Specifically, we can obtain

$$[\mathbf{J}_{\text{daisy}}^{-1}(\boldsymbol{\theta})]_{m,m} = \begin{cases} m\rho_b, & m \in [1, M-1] \\ (m-M+1)\rho_a, & m \in [M, 2M-2] \end{cases}. \quad (10)$$

where $\rho_b := \sigma_n^2/(b^2|h|^2)$ and $\rho_a := \sigma_n^2/(a^2|h|^2)$.

For an arbitrary effective interconnection strategy with $(M-1)$ transmission lines, the interconnection network can be decoupled into a set of daisy chain interconnection subnetworks. For example, the interconnection network in Fig. 3 can be decoupled into three daisy chain interconnection subnetworks as shown in Fig. 4. Since α_f , β_f , and h are assumed to be known, the CRLBs for α_m and β_m are determined by the calibration path of the m -th antenna and the SNR in the corresponding measurements. Hence, the CRLBs for the calibration coefficients of an arbitrary interconnection strategy can be obtained by computing the CRLBs with the decoupled daisy chain interconnection subnetworks independently. Note the CRLBs with each subnetwork can be directly obtained with the results in (10). We call the number of antennas along the calibration path of an ordinary antenna excluding the reference antenna as the ‘‘calibration distance’’. Let d_m denote the calibration distance of the m -th antenna. According to the results in (10), under AS-1 and AS-2, for an arbitrary effective interconnection strategy, the CRLBs for α_m and β_m , $\forall m \neq f$, can be derived as

$$\text{CRLB}(\alpha_m) = d_m\rho_b, \quad \text{CRLB}(\beta_m) = d_m\rho_a. \quad (11)$$

Meanwhile, for an arbitrary effective interconnection strategy, according to the results in (11), the average CRLBs for $\boldsymbol{\alpha}$ and $\boldsymbol{\beta}$ can

be obtained as follows:

$$\text{CRLB}(\boldsymbol{\alpha})_{\text{Average}} = \bar{d}\rho_b, \quad \text{CRLB}(\boldsymbol{\beta})_{\text{Average}} = \bar{d}\rho_a, \quad (12)$$

where $\bar{d} := \sum_{m=1}^{M-1} d_m/(M-1)$ represents the average calibration distance. In particular, for the star interconnection strategy, i.e. all the ordinary antennas are directly interconnected to the reference antenna, the average calibration distance $\bar{d} = 1$. This shows that the star interconnection achieves the smallest average CRLB. In summary, we can establish the following result.

Proposition 1. *Considering a BS with M antennas interconnected with $(M-1)$ transmission lines, assuming only total $2(M-1)$ measurements are available, under AS-1 and AS-2, the star interconnection minimizes the average CRLB for all the unknown calibration coefficients during internal self-calibration.*

Proposition 1 indicates the star interconnection strategy is the optimal interconnection when the BS has $2(M-1)$ measurements. In next section, we will analyze the optimality of the daisy chain interconnection strategy under limited time resources.

4. OPTIMALITY OF THE DAISY CHAIN

As mentioned in [7], the daisy chain interconnection strategy requires fewer time resources to collect the $2(M-1)$ measurements. However, the authors in [7] only demonstrated that the daisy chain interconnection could outperform the star interconnection with numerical simulations. In this section, we will prove the optimality of the daisy chain interconnection and the corresponding condition.

When $M = 2$, there is only one unique interconnection strategy. In the following analyses, it is thus assumed that $M \geq 3$. To characterize the constraint on the time resources, we assume that each measurement of the sounding signal consumes T seconds. To obtain $2(M-1)$ measurements, with the star interconnection strategy, we need $T_{\text{star}} = 2(M-1)T$ seconds. However, with the daisy chain interconnection strategy, we only need $T_{\text{daisy}} = 4T$ seconds to collect the same amount of measurements due to the fact that these measurements can be performed in parallel [7]. Consider an arbitrary effective interconnection strategy with $(M-1)$ transmission lines. Let N_m be the number of antennas that directly interconnected to the m -th antenna. Define $N_{\text{max}} := \max\{N_m | m = 1, \dots, M\}$. Note that $2 \leq N_{\text{max}} \leq M-1$ when $M \geq 3$. To obtain $2(M-1)$ measurements, we need at least $2N_{\text{max}}T$ seconds. It can be observed that $N_{\text{max}} = 2$ if and only if the interconnection is the daisy chain interconnection. Further, we see $N_{\text{max}} = M-1$ if and only if the interconnection is the star interconnection. We can first have the following proposition summarizing our findings.

Proposition 2. *For a BS with $M \geq 3$ antennas interconnected with $(M-1)$ transmission lines, we need T_{arb} seconds to obtain $2(M-1)$ calibration measurements with an arbitrary interconnection strategy. The required time T_{arb} satisfies the following condition:*

$$4T \leq T_{\text{arb}} \leq 2(M-1)T, \quad (13)$$

where the first equality holds if and only if the interconnection is the daisy chain interconnection, and the second equality holds if and only if the interconnection is the star interconnection.

Assume that the BS has a total budget of $T_{\text{star}} = 2(M-1)T$ seconds to collect the calibration measurements. For an arbitrary effective interconnection strategy, we can utilize the additional $T_d := (T_{\text{star}} - T_{\text{arb}})$ seconds to acquire additional measurements. Define

$I := \lfloor \frac{T_{\text{star}}}{T_{\text{arb}}} \rfloor \geq 1$ and $F := \text{mod}(T_{\text{star}}, T_{\text{arb}})$. In the following derivations, it is assumed that $(I - 1)T_{\text{arb}}$ seconds are used to obtain additional $(I - 1)$ independent $2(M - 1)$ measurements for all the unknown calibration coefficients and the remaining F seconds are not considered¹. As a result, the average CRLBs for α and β with an arbitrary effective interconnection strategy are given by

$$\text{CRLB}(\alpha)_{\text{Average}} = \rho_b \bar{d}/I, \text{CRLB}(\beta)_{\text{Average}} = \rho_a \bar{d}/I. \quad (14)$$

According to Proposition 2, the daisy chain interconnection strategy consumes the least amount of time resources to collect the measurements and the additional time resources can be utilized to improve the calibration performance. For the daisy chain interconnection strategy, as defined in (12), the average calibration distance \bar{d} is given by

$$\bar{d} = \frac{(M - 2f)}{2} + \frac{(f - 1)^2}{M - 1} + 1. \quad (15)$$

Meanwhile, we have $I = \lfloor \frac{(M-1)}{2} \rfloor$ when $2(M - 1)T$ seconds are available to acquire the $2(M - 1)$ calibration measurements. Note that the average calibration distance \bar{d} in (15) is minimized when $f = \frac{M+1}{2}$. Accordingly, the average CRLB is minimized when $f = \lfloor \frac{M+1}{2} \rfloor$ for the daisy chain interconnection strategy. Now we can establish the following results.

Proposition 3. For a BS with M antennas interconnected with $(M - 1)$ transmission lines, assuming total $2(M - 1)T$ seconds are available to acquire the $2(M - 1)$ calibration measurements, under AS-1 and AS-2, the daisy chain interconnection strategy gives the best calibration performance when $f = \lfloor \frac{M+1}{2} \rfloor$. The corresponding average CRLBs are

$$\text{CRLB}(\alpha)_{\text{Average}} = \rho_b \bar{d}/I, \text{CRLB}(\beta)_{\text{Average}} = \rho_a \bar{d}/I, \quad (16)$$

where $\bar{d}/I = (M + 1)/(2M - 2)$ when M is odd and $\bar{d}/I = (M^2)/(2M^2 - 6M + 4)$ when M is even.

From Proposition 3, we see $\bar{d}/I < 1$ when $M \geq 5$. In other words, the daisy chain interconnection outperforms the star interconnection when $M \geq 5$. Further, it can be seen that the value of \bar{d}/I becomes smaller as the number of antennas increases when $M \geq 5$. As $M \rightarrow \infty$, for the daisy chain interconnection strategy, the asymptotic average CRLBs for α and β are given by

$$\lim_{M \rightarrow \infty} \text{CRLB}(\alpha)_{\text{Average}} = \rho_b/2, \lim_{M \rightarrow \infty} \text{CRLB}(\beta)_{\text{Average}} = \rho_a/2. \quad (17)$$

These asymptotic average CRLBs are just half of the corresponding results for the star interconnection strategy. The above results show that, with a total budget of $2(M - 1)T$ seconds for calibration, the daisy chain interconnection strategy outperforms the star interconnection when $M \geq 5$. The relative performance gain decreases as M goes large and the average CRLBs are bounded by (17).

5. NUMERICAL RESULTS

In this section, numerical results are provided to verify our analytical results. In our simulations, we compare the star interconnection and the daisy chain interconnection for self-calibration at the BS. In order to align with our analytical CRLBs in (11), we assume that the RF gains of the reference antenna, i.e. α_f and β_f , are given and fixed. In the meantime, the interconnection channel h is also

¹The remaining F seconds can further be used to improve the total calibration performance, and the effects of the remaining F seconds can also be analyzed with similar methods in the paper.

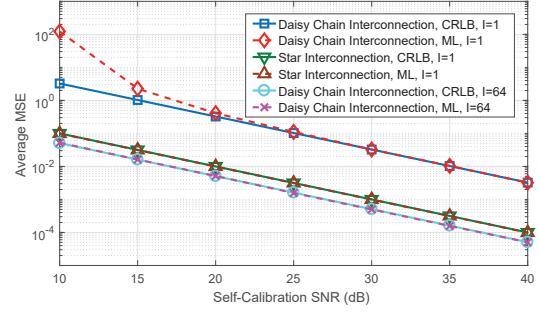


Fig. 5. Full calibration for different interconnection strategies. (“Star Interconnection”: star interconnection strategy is used for full calibration at the BS; “Daisy Chain Interconnection”: daisy chain interconnection is used for full calibration at the BS; “CRLB”: average CRLB over all the unknown calibration coefficients; “ML”: simulated average MSE of all the estimated calibration coefficients for different interconnection strategies with the maximum-likelihood (ML) estimator; Symbol I in the legend means $2I(M - 1)$ independent measurements are obtained.)

assumed to be known. Note the interconnection channel h is time-invariant and can be estimated in advance. Then we can obtain the ML estimates of the calibration coefficients, i.e. α_m and β_m , for any effective interconnection strategy implemented at the BS. Some key parameters assumed in the simulations are listed as follows.

- The number of antennas at the BS is set to $M = 129$;
- The amplitudes of the transmit and receive RF gains are equal to 1, i.e. $|\alpha_m| = |\beta_m| = 1, \forall m \in [1, M]$. The phases of the RF gains are uniformly distributed within $[-\pi, \pi]$;
- The transmitted sounding signal is equal to 1;
- The reference antenna is the 64-th antenna, i.e. $f = 64$;
- The SNR in the calibration measurements varies from 10dB to 40dB.

In Fig. 5, the average CRLB and the simulated average mean-square-error (MSE) of all unknown calibration coefficients are compared under different constraints. The results show that the star interconnection outperforms the other interconnection strategies when $I = 1$, i.e. $2(M - 1)$ calibration measurements are available. However, when we have $2(M - 1)T$ seconds time resources, the daisy chain interconnection strategy shows better calibration performance than the star interconnection strategy.

6. CONCLUSIONS

In this paper, we have studied the interconnection strategy for internal self-calibration in massive MIMO systems. Based on the derived CRLBs for the unknown calibration coefficients, on the one hand, we have shown that the star interconnection is the optimal strategy to interconnect the antennas at the BS for internal self-calibration when the BS has $2(M - 1)$ measurements. On the other hand, when the number of antennas becomes large, the daisy chain interconnection outperforms the star interconnection when the BS only has $2(M - 1)T$ seconds to collect the calibration measurements.

7. REFERENCES

- [1] E. G. Larsson, O. Edfors, F. Tufvesson, and T. L. Marzetta, "Massive MIMO for next generation wireless systems," *IEEE Commun. Mag.*, vol. 52, no. 2, pp. 186–195, Feb. 2014.
- [2] G. S. Smith, "A direct derivation of a single-antenna reciprocity relation for the time domain," *IEEE Trans. Antennas Propag.*, vol. 52, no. 6, pp. 1568–1577, Jun. 2004.
- [3] X. Luo, "Multiuser massive MIMO performance with calibration errors," *IEEE Trans. Wireless Commun.*, vol. 15, no. 7, pp. 4521–4534, Jul. 2016.
- [4] W. Zhang, H. Ren, C. Pan, M. Chen, R. C. Lamare, B. Du, and J. Dai, "Large-scale antenna systems with UL/DL hardware mismatch: Achievable rates analysis and calibration," *IEEE Trans. Commun.*, vol. 63, no. 4, pp. 1216–1229, Apr. 2015.
- [5] H. Wei, D. Wang, H. Zhu, J. Wang, S. Sun, and X. You, "Mutual coupling calibration for multiuser massive MIMO systems," *IEEE Trans. Wireless Commun.*, vol. 15, no. 1, pp. 606–619, Jan. 2016.
- [6] C. Shepard, H. Yu, N. Anand, L. E. Li, T. Marzetta, R. Yang, and L. Zhong, "Argos: Practical many-antenna base stations," in *Proc. ACM Int. Conf. Mobile Comput. Netw. (Mobicom)*, Istanbul, Turkey, Aug. 2012, pp. 1–12.
- [7] A. Benzin and G. Caire, "Internal self-calibration methods for large scale array transceiver software-defined radios," in *Proc. IEEE Int. ITG Workshop Smart Antennas*, Berlin, Germany, Mar. 2017, pp. 1–8.
- [8] K. Nishimori, K. Cho, Y. Takatori, and T. Hori, "Automatic calibration method using transmitting signals of an adaptive array for TDD systems," *IEEE Trans. Veh. Technol.*, vol. 50, no. 6, pp. 1636–1640, Nov. 2001.
- [9] J. Liu, G. Vandersteen, J. Craninckx, M. Libois, M. Wouters, F. Petr e, and A. Barel, "A novel and low-cost analog frond-end mismatch calibration scheme for MIMO-OFDM WLANs," in *Proc. IEEE Radio Wireless Symp.*, San Diego, CA, Oct. 2006, pp. 219–222.
- [10] J. Vieira, F. Rusek, O. Edfors, S. Malkowsky, L. Liu, and F. Tufvesson, "Reciprocity calibration for massive MIMO: Proposal, Modeling, and Validation," *IEEE Trans. Wireless Commun.*, vol. 16, no. 5, pp. 3042–3056, May 2017.
- [11] F. Kaltenberger, H. Jiang, M. Guillaud, and R. Knopp, "Relative channel reciprocity calibration in MIMO/TDD systems," in *Proc. IEEE Future Netw. Mobile Summit*, Florence, Italy, Jun. 2010, pp. 1–10.
- [12] J. Shi, Q. Luo, and M. You, "An efficient method for enhancing TDD over the air reciprocity calibration," in *Proc. IEEE Wireless Commun. Networking Conf.*, Cancun, Quintana Roo, Mar. 2011, pp. 339–344.
- [13] R. Rogalin, O. Y. Bursalioglu, H. Papadopoulos, G. Caire, A. F. Molisch, A. Michaloliakos, V. Balan, and K. Psounis, "Scalable synchronizaiton and reciprocity calibration for distributed multiuser MIMO," *IEEE Trans. Wireless Commun.*, vol. 13, no. 4, Apr. 2014.
- [14] X. Luo, "Robust large scale calibration for massive MIMO," in *Proc. IEEE Global Commun. Conf. (GLOBECOM)*, San Diego, CA, Dec. 2015, pp. 1–6.
- [15] S. M. Kay, *Fundamentals of Statistical Signal Processing: Estimation Theory*. Upper Saddle River, New Jersey, USA: Prentice Hall, 1993.